Available online at www.sciencedirect.com

ScienceDirect

IFAC PapersOnline CONFERENCE PAPER ARCHIVE

IFAC PapersOnLine 58-25 (2024) 114–119

Stability-Constrained Contingency Analysis for Modern Power Systems

Rajan Ratnakumar[1, 3] and Ganesh K. Venayagamoorthy[1, 2, 4]

[1]*Real-Time Power and Intelligent Systems Laboratory, Holcombe Department of Electrical and Computer Engineering, Clemson University, Clemson, SC 29634, USA.*

[2]*Department of Electrical, Electronic and Computer Engineering, University of Pretoria, South Africa.*

[3](rratnak@g.clemson.edu).

[4](gkumar@ieee.org).

Abstract: Modern power systems comprise diverse nonlinear components, and an increasingly large number of low inertia renewable power sources necessitate the modernization of conventional power system security measures. Contingency analysis (CA), a routine process for power system operators, ensures grid security under unforeseen circumstances by identifying potential issues and enabling proactive measures for uninterrupted power flow. Electromechanical oscillations (EMOs) in the power system that are a threat to stability must be regularly monitored and mitigated. An online hierarchical EMO index integrating time and frequency response analysis can be utilized for system stability assessment. The integration of an EMO index threshold into contingency analysis is presented in this paper to enhance system security. This new approach is referred to as the stability-constrained contingency analysis (SCCA). Typical results for a modified two-area, four-machine power system with large solar photovoltaic plants simulated on a real-time digital simulator (RTDS) are presented. These results demonstrate that SCCA flags potential issues that can arise from EMOs for certain contingencies, whereas traditional CA does not, as it solely considers bus voltage limits and line ratings.

Keywords: Contingency analysis, electromechanical oscillations, security, stability.

1. INTRODUCTION

The interconnected power system of today is dynamic, complex, and made up of a variety of nonlinear parts that can generate, transfer, and distribute electrical energy over broad geographical regions. As a result of the need for clean, sustainable, and environmentally friendly power sources, the penetration of renewable energy is rapidly increasing in the modern power system. Power system security is increasingly challenged by the integration of low-inertia renewable energy sources into the transmission grid (Song et al., 2023). Therefore, it is important to modernize the conventional power system security measures to guarantee secure power system operations.

Contingency analysis (CA) in power systems is carried out by the system operator periodically to ensure the security and reliability of the grid under various unforeseen circumstances or operational contingencies. CA in modern power systems involves power system models to simulate the effects of potential equipment failures. CA incorporates parameters such as bus voltages, power generation levels, loads and power interchanges to identify and assess potential overloads, violations and critical situations in power systems. This enables CA to support both system planning and real-time decision-making and dispatch by system operators (EPRI, 2010).

Generally, CA will flag which line or generation outages will cause power flows or voltages to violate the specified limits. CA in the power system focuses on *N*-1 contingencies, ensuring that the grid remains secure even in the event of the most severe single component or operational failure (Wood, A. J et al., 2012). The traditional may not be reliable for the modern power system with increasingly large number of low-inertia renewable power sources.

Enhanced methods have been proposed to improve traditional CA approaches, addressing specific challenges in system security. One notable advancement is the introduction of enhanced contingency analysis, which extended classical CA by incorporating static voltage analysis based on modal analysis (Bulat et al., 2021). This methodology provides a more comprehensive assessment, distinguishing safe operating conditions from potential voltage instability threats. A study on real-time transient stability assessment in power systems, utilizing the Prony method and transient energy function analysis, focused on practical generator maintenance scheduling and contributes valuable insights to electric energy management during contingencies in the Nigerian power system (Yare et al., 2010). The studies on transient stability-constrained optimal power flow (Abhyankar et al., 2017) provided valuable insights to power system analysis, complementing traditional CA by addressing dynamic stability challenges.

10.1016/j.ifacol.2024.10.247

As mentioned above, the incorporation of low-inertia renewable power sources makes the monitoring and damping of electromechanical oscillations (EMOs) in the power system crucial (Hauer et al., 2007; Zuo et al., 2019). Undamped EMOs can be detrimental to the secure operation of a power system. The stability of the power system is greatly impacted by disturbances, and EMOs can intensify following severe disturbances. Hence, it is crucial to consistently monitor and apply damping measures to ensure secure power system operation. Some contingencies may not violate the voltage limits and line ratings but can give rise to EMO(s) that has low damping. Therefore, integrating the EMO index-based stability assessment into contingency analysis is crucial for enhancing modern power system security.

An online hierarchical EMO index (EMOI, between 0 and 1) that integrates time response analysis (TRA) and frequency response analysis (FRA) was introduced in J. Richards et al. (2022) and is used to provide operational situational awareness (OpSA). Furthermore, the EMOI has been used for the design of a secondary load frequency controller to improve EMO damping (Ratnakumar et al., 2023). This index provides an indication and can be used to flag the level of security of a power system due to EMOs, especially from severe disturbances. In this paper, a new method for defining an EMOI based stability threshold that can be utilized in carrying out stability-constrained contingency analysis (SCCA) is presented.

The primary contributions of this paper are as follows:

- Derivation of an EMOI based stability threshold ($EMOI_{th}$) for modern power systems utilizing a new electromechanical oscillation index (EMOI).
- Development of a stability-constrained contingency analysis (SCCA) method for modern power systems utilizing EMOI based stability threshold.
- Implementation of the SCCA for a modified two-area, four-machine power system with two large solar photovoltaic plants simulated on a real-time digital simulator (RTDS). Typical results are presented to show the efficacy of the EMOI based SCCA over the traditional CA.

The rest of the paper is organized as follows: Section 2 describes the development of an EMOI-based stability-constrained contingency analysis and its implementation on a modified two-area, four-machine system with two solar photovoltaic plants. In Section 3, typical results and discussions are presented. Finally, the conclusion is presented in Section 4.

2. DEVELOPMENT OF THE EMOI-BASED SCCA

The development of derivation of the EMOI based stability threshold, SCCA, and the power system studied in this paper are described in the following subsections.

2.1 The EMOI Based Stability Threshold ($EMOI_{th}$)

The process of defining the EMOI based stability threshold is shown in Fig. 1. The EMO index (EMOI), between 0 and 1, based on phasor measurement unit (PMU) data, was developed in J. Richards et al. (2022), quantifying the severity of EMOs, with '0' representing the most severe/critical, in a power system, thus enabling an effective assessment of power system stability.

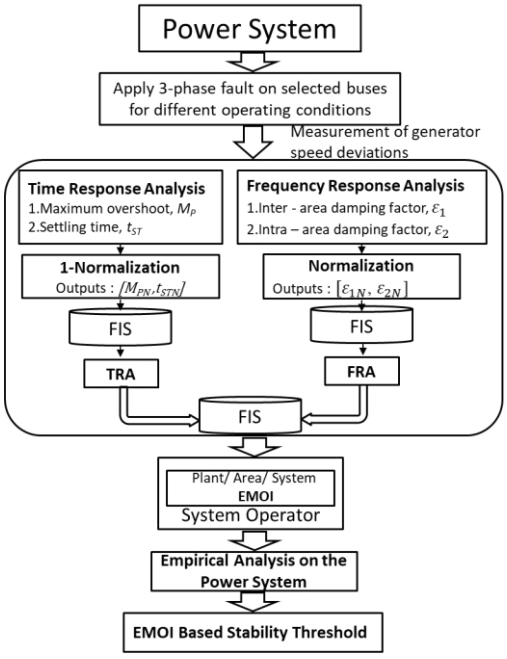

Figure 1 Schematic diagram to define the EMOI based stability threshold.

The TRA is obtained by using Takagi–Sugeno (TS) fuzzy logic, (1a), with two inputs, M_{PN} andt_{STN}, and nine simplified rules. Here, M_{PN} and t_{STN}, in (1b) and (1c), denote the normalized maximum overshoot and settling time, respectively, while M_P and t_{ST} represent their maximum actual values. NF_{MP} and $NF_{t_{ST}}$ stand for the associated normalization factors. (1-Normalization) is carried out because bigger values of maximum overshoot and settling time indicate worse conditions. Similarly, inter and intra-area damping factors of the signal is normalized, and the FRA is obtained using TS fuzzy logic, (2a), with two inputs, ε_{1N} andε_{2N}, and nine simplified rules. Here, ε_{1N} and ε_{2N} , in (2b) and (2c), denote, the normalized inter-area and intra-area damping factors, respectively, while ε_1 and $\varepsilon_2$represent their actual values. NF_{ε_1} and NF_{ε_2} stand for the associated normalization factors. The EMOI is obtained by integrating the estimated TRA and FRA components using TS fuzzy logic, (3). Since there are two input variables and three membership functions for each variable, as shown in Fig. 2, there are nine fuzzy rules for each of the three fuzzy engines, namely: TRA, FRA, and EMOI, as shown in Table 1.

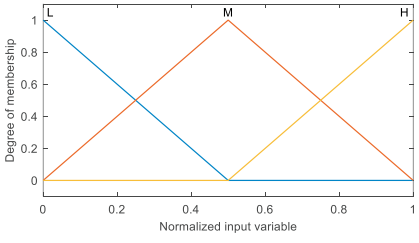

Figure 2 Input membership function used for computing TRA, FRA and EMOI.

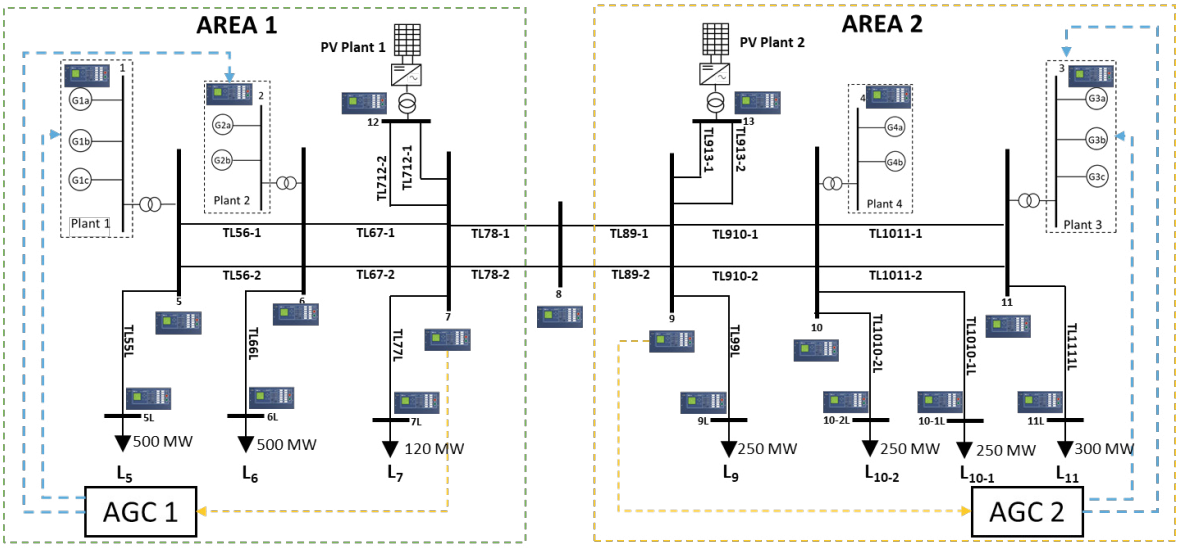

Figure 3 Modified two-area four-machine power system with two large solar photovoltaic plants and automatic generation controls (AGCs).

$$TRA = FIS(M_{PN}, t_{STN}) \quad (1a)$$

where,

$$M_{PN} = 1 - \frac{M_P}{NF_{M_P}} \quad (1b)$$

$$t_{STN} = 1 - \frac{t_{ST}}{NF_{t_{ST}}} \quad (1c)$$

$$FRA = FIS(\varepsilon_{1N}, \varepsilon_{2N}) \quad (2a)$$

where,

$$\varepsilon_{1N} = \frac{\varepsilon_1}{NF_{\varepsilon_1}} \quad (2b)$$

$$\varepsilon_{2N} = \frac{\varepsilon_2}{NF_{\varepsilon_2}} \quad (2c)$$

$$EMOI = FIS(TRA, FRA) \quad (3)$$

The rule firing strength equation and defuzzification for the implemented TS fuzzy logic are shown in (4) and (5). Here, x_1 and x_2 are the inputs, and F_1 and F_2 are the membership functions. w_i is the rule firing strength derived from the rule antecedent, z_i is the rule output level, and N is the number of rules.

$$w_i = AndMethod\big(F_1(x_1), F_2(x_2)\big) \quad (4)$$

$$Final\ output = \frac{\sum_{i=1}^{N} w_i z_i}{\sum_{i=1}^{N} w_i} \quad (5)$$

Table 1 Fuzzy rule set for TRA, FRA and EMOI

TRA Fuzzy Rules				FRA Fuzzy Rules				EMOI Fuzzy Rules			
Rule No.	M_{PN}	t_{stN}	Output	Rule No.	ε_{1N}	ε_{2N}	Output	Rule No.	*TRA*	*FRA*	Output
1	L	L	0	1	L	L	0	1	L	L	0
2	L	M	0.25	2	L	M	0.25	2	L	M	0.25
3	L	H	0.5	3	L	H	0.5	3	L	H	0.5
4	M	L	0.25	4	M	L	0.25	4	M	L	0.25
5	M	M	0.5	5	M	M	0.5	5	M	M	0.5
6	M	H	0.75	6	M	H	0.75	6	M	H	0.75
7	H	L	0.5	7	H	L	0.5	7	H	L	0.5
8	H	M	0.75	8	H	M	0.75	8	H	M	0.75
9	H	H	1	9	H	H	1	9	H	H	1

The process to obtain the $EMOI_{th}$ involves testing the system by applying three-phase 10 cycles faults at selected buses and evaluating the EMOIs. These tests are carried out at different operating conditions and contingencies. The $EMOI_{th}$ can be adjusted according to the degree of stringency. The System EMOIs characteristics with TRA and FRA for the modified two-area four-machine power system depicted in Fig. 3 are presented in Fig. 4. This plot presents 86 points from three-phase, 10-cycle fault tests: 20 EMOIs for five buses with PSS ON/OFF and 66 EMOIs for faults placed at Bus 8 with 23 line contingencies and 10 generator contingencies at two operating tie-line flows, 400 MW and 200 MW.

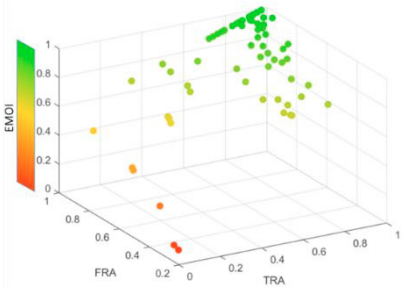

Figure 4 Visualization of System EMOIs based on their corresponding TRA and FRA values for a modified two-area, four-machine power system.

2.2 SCCA

The stability assessment is carried out for every *N*-1 generation and line outage contingencies in the system like, it is carried out to assess any voltage limit or line overloading violation. The operator is alarmed in case of any abnormal EMO conditions that might occur, like it is done with voltage limit and line rating violations. The SCCA flowchart is depicted in Fig. 5. The main difference from the traditional CA is the inclusion of stability assessment as a crucial component. Every contingency is assessed for EMOI determination. The system's stability is evaluated by calculating the EMOI for each contingency. Based on this value, the system's status will be classified as either normal or critical according to the pre-defined EMOI stability threshold. If the EMOI is in the critical zone, below the threshold, an alarm is triggered to alert the operator. The operator has then to carry out a security-constrained optimal power flow to prevent this critical and

insecure state from occurring in the event of a contingency. This comprehensive approach ensures that stability is prioritized and closely monitored throughout the CA process, providing a robust framework for maintaining secure and reliable modern power system operation.

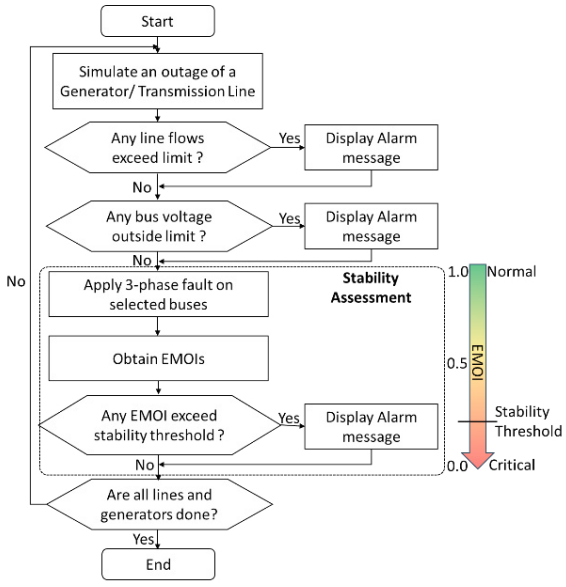

Figure 5 Flowchart of the SCCA.

2.3 Modified Two-Area, Four-Machine Power System

The modified two-area, four-machine power system (Kundur, 1994) was used as the test power system to demonstrate the SCCA and was simulated on the real-time digital simulator (RTDS). The power system has four power plants, including ten generators and two large solar photovoltaic power plants in two areas. The solar PV plants in Area 1 and Area 2 have a rating of 150 MWp each. Table A.1 displays the power plants' ratings, generation, and operational conditions for two different tie-line power transfer scenarios. The generation of Areas 1 and 2 is regulated by automatic generation controllers, AGC 1 and AGC 2, respectively.

3. RESULTS AND DISCUSSION

The SCCA is implemented on the modified two-area, four-machine power system (Fig. 3) to demonstrate its importance for modern power system operations. The stability assessment loop is carried out for each transmission line and generator contingency, and the results are recorded. The EMOIs are obtained by applying a three-phase 10-cycle fault at Bus 8. The damping normalizing factors are defined as 0.25 (25%). The normalization factors for the maximum overshoot and settling time are determined through the calibration process. The EMOI threshold value is selected as 0.5. The bus voltages and line power flows remained within acceptable limits for all evaluated contingencies, confirming secure operation of the power system according to traditional CA standards. However, stability assessments carried out with the SCCA unveiled stability issues for certain contingencies, which can be detrimental to secure operation of the power system.

Fig. 6(a) illustrates the TRA characteristics of Plant 1 with the normalized maximum overshoot and settling time obtained for all line and generator contingencies. In Fig. 6(b), the FRA characteristics of Plant 1 are depicted with normalized inter-area and intra-area damping for all line and generator contingencies. Figs. 7 (a), (b) and (c) illustrate the EMOI characteristics with TRA and FRA and passed/ failed contingencies according to different $EMOI_{th}$ values. The instances shown in red indicate the potential issue identified by the SCCA that was overlooked by traditional CA.

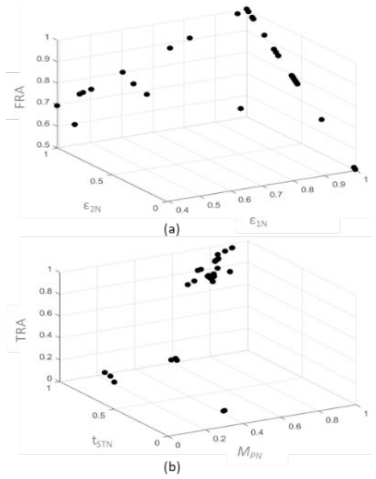

Figure 6 Visualization of Plant 1: (a) TRA vs. normalized maximum overshoot and settling time (b) FRA vs. normalized inter-area damping and intra area damping for the line and generator contingencies.

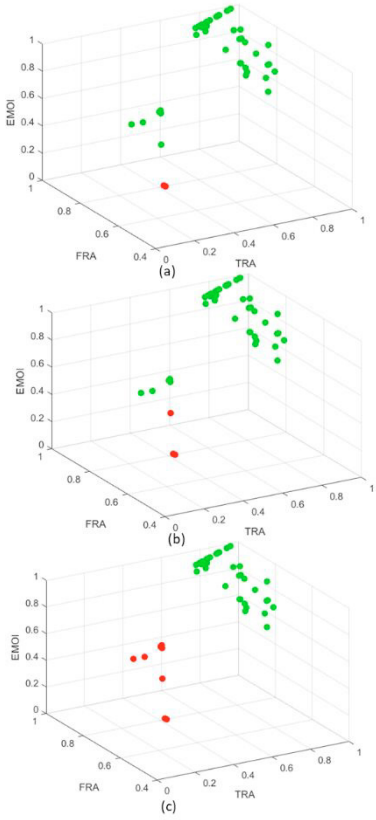

Figure 7 Visualization of Plant 1 EMOI vs. TRA and FRA. Line and generator contingencies are categorized as 'Pass' or 'Fail', green/ red, respectively, based on different EMOI thresholds, namely: (a) 0.4, (b) 0.5 and (c) 0.6.

3.1 Transmission Line Contingencies

The assessment of transmission line contingencies is carried out by isolating each line individually and subsequently subjecting the system to a three-phase 10 cycles fault at Bus 8. Fig. 7 (b) shows the TRA and FRA of the assessments and the passed and failed contingencies for different EMOI thresholds. The results provide valuable insights into the system's behavior during contingencies. From the EMOIs, it is apparent that certain line contingencies have a more pronounced impact on the system, especially when the tie-line flow is at 400 MW. Removing transmission lines TL89-1, TL89-2, TL99L, TL1010-1L, and TL1010-2L, with a tie-line flow of 400 MW, significantly decreases EMOIs, potentially driving the system towards a critical condition during the fault. Other cases exhibit changes in EMOI but still fall within the secure range.

Fig. 8 displays the speed deviation of Plant 1 for a similar type of fault with and without line TL89-1 (tie-line: 200 MW). The results show a reduction in EMOI, but the system remains within secure operating conditions.

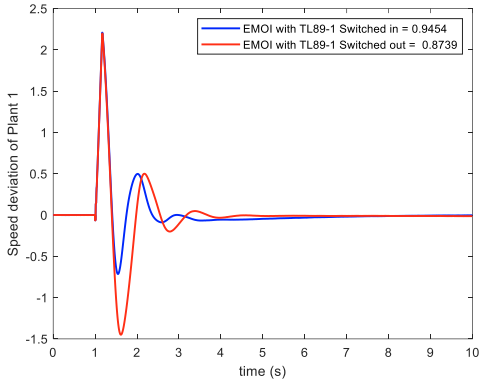

Figure 8 Speed deviation of Plant 1 with 3-phase 10 cycles fault at Bus 8 with and without TL89-1 (Tie-line: 200 MW).

Fig. 9 illustrates the speed deviation of Plant 1 during a three-phase 10 cycles fault at Bus 8, with and without line TL89-1 (tie-line: 400 MW). The tie-line power is maintained at 400 MW, but operational conditions shift due to load changes. The results show that the EMOI has decreased beyond the threshold and is unstable indicating that the system is in a critical stage in this contingency.

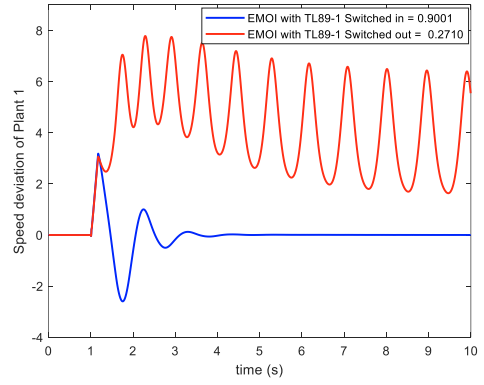

Figure 9 Speed deviation of Plant 1 with 3-phase 10 cycles fault at Bus 8 with and without TL89-1 (Tie-line: 400 MW).

3.2 Generator Contingencies

The study of generator contingencies is carried out by isolating each generator one by one and subjecting the system to a three-phase 10 cycle-fault at Bus 8, the same as it was done in the transmission line contingency analysis. Fig.7 illustrates the TRA and FRA assessments alongside passed and failed contingencies based on the determined EMOI thresholds The outage of generators in Area 1 has a greater impact on stability compared to the outage of generators in Area 2 during 400 MW tie-line interchange. The EMOI for these contingencies is beyond the stability threshold. Fig. 10 illustrates the speed deviation of Plant 1 for the same fault scenario mentioned earlier, when the generator G2a (tie-line 200 MW) is switched ON and OFF. The outage of this generator appears to be a more critical scenario due to its larger capacity. The results indicate a decline in EMOI, yet the system stays within a secure operational state. The change in the operation conditions of the generators is shown in Table A.1. Fig. 11 depicts the speed deviation of Plant 1 for a three-phase 10 cycles fault initiated at Bus 8 under two conditions: with generator G1c switched ON and OFF (with a tie-line power flow of 400 MW). The EMOI has fallen below the threshold, signaling the system's critical state for this generator contingency. The change in the operation conditions of the generators is shown in Table A.1.

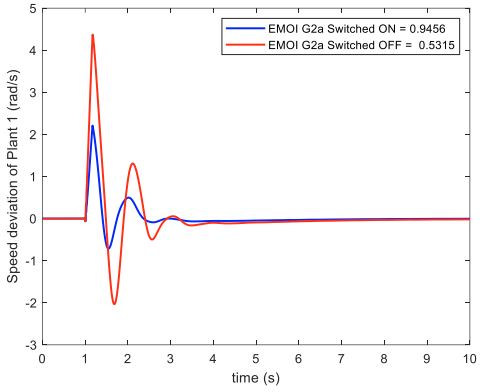

Figure 10 Speed deviation of Plant 1 with 10 cycles fault at Bus 8 with and without G2a (Tie-line: 200 MW).

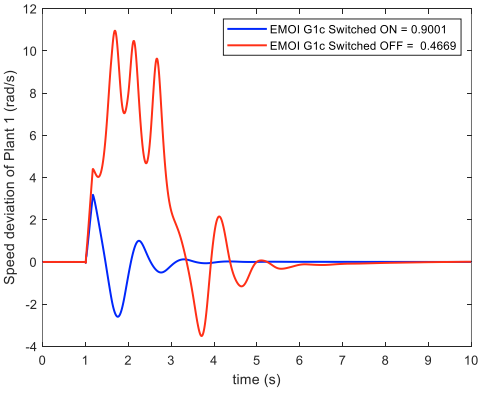

Figure 11 Speed deviation of Plant 1 with 10 cycles fault at Bus 8 with and without G1c (Tie-line: 400 MW).

Table 2 shows a comparison of the traditional CA and the SCCA. It can be observed that the SCCA flags potential issues that can arise from EMOs for certain line and generator

contingencies. However, traditional CA fails to identify these as it is solely based on bus voltage limits and line ratings.

Table 2 Comparison of traditional CA and SCCA with 0.5 EMOI threshold

Contingency	EMOI	Traditional CA	SCCA
TL89-1 (Tie-line: 200 MW)	0.8739	Pass	Pass
TL89-1 (Tie-line: 400 MW)	0.2710	Pass	Fail
G2a (Tie-line: 200 MW)	0.5315	Pass	Pass
G1c (Tie-line: 400 MW)	0.4669	Pass	Fail

4. CONCLUSION

The modern power system is evolving with increasingly large number of low-inertia renewable power sources. Thus, monitoring and mitigating electromechanical oscillations has become paramount. Unlike traditional contingency analysis, which is primarily based on bus voltage limits and line ratings, utilizing the electromechanical oscillation index (EMOI) in stability-constrained contingency analysis (SCCA) provides a more comprehensive assessment. The SCCA was successfully implemented for a modified two-area four-machine system with two large solar photovoltaic plants, demonstrating its effectiveness as a valuable stability indicator in ensuring the secure operation of modern power systems. The SCCA flags potential issues that may arise from EMOs during contingencies, whereas traditional CA does not. The integration of a rather simple and easy-to-implement stability indicator, the EMOI, into contingency analysis, represents a relevant advancement in the security assessment of modern power systems.

ACKNOWLEDGEMENT

This research was funded by US NSF grants (CNS 2131070, ECCS 2234032, and CNS 2318612) and the Duke Energy Distinguished Professor Endowment Fund.

REFERENCES

Abhyankar, S., Geng, G., Anitescu, M., Wang, X., & Dinavahi, V. (2017). Solution techniques for transient stability-constrained optimal power flow–Part I. *IET Generation, Transmission & Distribution*, 11(12).

Bulat, H., Franković, D., & Vlahinić, S. (2021). Enhanced contingency Analysis—A power system operator tool. *Energies*, 14(4).

EPRI (2010). Contingency analysis – baseline

Hauer, J. F., Trudnowski, D. J., & DeSteese, J. G. (2007). A perspective on WAMS analysis tools for tracking of oscillatory dynamics. In *Proceedings of the 2007 IEEE Power Engineering Society General Meeting*, 1-10.

Zuo, J., Tang, J., Guo, H., Hu, D., Zhang, K., & Xiang, M. (2019). Low-frequency oscillation mode identification with OpenPDC platform. In *Proceedings of the 2019 6th International Conference on Systems and Informatics (ICSAI)*, 223-227.

Kundur, P. S., & Malik, O. P. (2022). *Power system stability and control (2nd ed.)*. McGraw-Hill Education, New York.

Ratnakumar, R., & Venayagamoorthy, G. K. (2023). Adaptive automatic generation control for improved stability of power systems with utility-scale photovoltaic plants. In *Proceedings of the 2023 IEEE IAS Global Conference on Renewable Energy and Hydrogen Technologies (GlobConHT)* (pp. 1-6).

Ratnakumar, R., Richards, J., & Venayagamoorthy, G. K. (2023). Modern control center operational situational awareness considering electromechanical oscillations. In *Proceedings of the 2023 IEEE Africon* (pp. 1-6).

Richards, J., Ratnakumar, R., & Venayagamoorthy, G. K. (2022). An online electromechanical oscillation index for a modern bulk power system. In *Proceedings of the CIGRE US National Committee, Grid of the Future Symposium*.

Song, J., Zhou, X., Zhou, Z., Wang, Y., Wang, Y., & Wang, X. (2023). Review of low inertia in power systems caused by high proportion of renewable energy grid integration. *Energies*, 16(16).

Wood, A. J., & Wollenberg, B. F. (2012). *Power generation, operation, and control*. Wiley, Hoboken, NJ, USA.

Yare, Y., & Venayagamoorthy, G. K. (2010). Real-time transient stability assessment of a power system during energy generation shortfall. In *Proceedings of the 2010 Innovative Smart Grid Technologies (ISGT)* (pp. 1-9).

Appendix A

Table A.1. Generation data

Area			Area 1 (MW)						Area 2 (MW)					
Plant			Plant 1			Plant 2		PV 1	Plant 3			Plant 4		PV 2
Generator			G1a	G1b	G1c	G2a	G2b		G3a	G3b	G3c	G4a	G4b	
Rating (MVA)			300	300	300	500	450	150	270	300	330	450	450	150
Inertia H(s)			3	3	3	2.7	3.7	-	4.13	3.3	3	2.65	2.65	-
Generation (MW)	Tie-line 200 MW	No Contingency	200	200	200	339	261	136	120	120	120	180	180	136
		Outage of G2a	273	273	273	0	381	136	120	120	120	180	180	136
	Tie-line 400 MW	No Contingency	235	235	235	391	313	136	88	88	88	133	133	136
		Outage of TL1010-1L	235	235	235	391	313	136	47	47	47	70	70	136
		Outage of G1c	282	282	0	462	384	136	88	88	88	133	133	136